



# Nano Science and Nano Technology

*An Indian Journal*

*Full Paper*

NSNTAIJ, 9(6), 2015 [204-214]

## Micro-hardness & thermal characterization of epoxy/ ABS blend reinforced with MgO nanocomposites

Ali A.M.Yassene<sup>1\*</sup>, M.Abd El-Rahman<sup>2</sup>

<sup>1</sup>Department of Radiation chemistry, National Center of Radiation Research and Technology NCRRT, Atomic Energy Authority, Cairo, (EGYPT)

<sup>2</sup>Department of Radiation Physics, National Center of Radiation Research and Technology NCRRT, Atomic Energy Authority, Cairo, (EGYPT)

E-mail: aliyasen76@yahoo.com

### ABSTRACT

In this study, acrylonitrilebutadiene styrene copolymer (ABS, 5 wt%) has been dissolved at 180 °C in an epoxy resin based on diglycidyl ether of bisphenol-A, DGEBA, different ratio (3, 5, 7, 10 wt %) of MgO nanoparticles were added to mixture, it has been irradiated with Gamma radiation at (20 and 50 kGy), then the epoxy component has been cross-linked with diamine hardeners. The micro-hardness, thermal analysis (TGA and DSC) and XRD of epoxy/ ABS nanocomposites had been investigated. The results indicated that, the micro-hardness, thermal stability and glass transition temperature ( $T_g$ ) of unirradiated no composite increased with increasing MgO load. Also, at the same MgO percentage, the irradiated specimens at 20 kGy were gave best result to micro-hardness properties. Finally, The X-ray diffraction patterns obtained for the systems confirmed the nanodispersion of MgO in the epoxy/ABS networks. It can be seen that, the addition of magnesium oxide particles to the polymer composites and the exposure to gamma radiation is working to increase the crystallization of epoxy/ABS blend.

© 2015 Trade Science Inc. - INDIA

### KEYWORDS

Epoxy;  
MgO;  
Blend;  
Radiation.

### INTRODUCTION

With the advance of science and technology, high-molecular weight materials become one of most attractive resources for advanced applications. Among them, epoxy resin is the most important in industry owing to its light weight, higher density, viscosity, excellent thermal stability, and cost effectiveness. However, its application range is limited because of its brittleness<sup>[1]</sup>. Among the existing modified pro-

cesses, rubber-toughened epoxy resins lead to degraded strength and rigidity of materials and hence no significance in fiber composite applications<sup>[2]</sup>. An alternative approach to toughen epoxy polymers for fiber composite applications is the use of epoxy blend as matrix with high performance thermoplastics<sup>[3-6]</sup>. Most of the studies on thermoplastic/thermoset blends are mainly focused on their mechanical properties and final morphologies. Recently, other authors have investigated the effect of the modifier

on the kinetics of curing<sup>[7-9]</sup>.

The effects of ionizing radiation on polymers and organic materials have been studied for many years<sup>[10-11]</sup>. It is well known that ionizing radiation induced processes does not need thermal activation, as the formation of reactive species does not present high values of activation energy. The possibility to work at room temperature represents one of the most attractive features of radiation curing of epoxies for production of advanced composites. These may due to the energy saving, the low emission of volatile species and the possibility to improve the mechanical properties of the materials because of the reduced thermal stresses<sup>[12-14]</sup>.

Gamma irradiation effect and ABS loading on curing and thermo- mechanical properties of epoxy/ ABS blends have been discussed in detail in our earlier studies<sup>[15]</sup>. The main objective of this study is to investigate the effect of Gamma radiation and MgO loading on epoxy/ ABS blend matrix. The microhardness, thermal properties and XRD of hybrid composites were investigated as a function of MgO composition. The relationship between the irradiation treatment and the thermo-mechanical properties of hybrid composites has been established.

## MATERIALS AND EXPERIMENTAL

### Materials

The studied system is based on a commercial epoxy [diglycidyl ether of bisphenol A], (KEMAPOXY 150), from chemicals for modern building international (CMB) Co., with epoxide equivalence weight in the range of 182–196 g/equiv and density at 25 oC (1.11 g/cm<sup>3</sup>). The curing agent used was cycloaliphatic amine, 4,4'-Diamino 3,3'-dimethyl dicyclohexyl methane, [3 DCM], supplied by (CMB).

Polyacrylonitrile-butadiene-styrene (ABS) powder, with density 1.04 g/ml at 25 oC and M. Wt 211.3 g/ mol was obtained from Sigma – Aldrich Co. P.N (180882). Figure 1 shows the chemical structures and reaction mechanisms of the samples.

### Preparation of epoxy/ABS blend

ABS polymer (5 wt %) was dissolved in epoxy resin at 180 °C for 15 min. then the epoxy / ABS mixture was cooled to room temperature, Afterward, the epoxy / ABS mixture was irradiated with Gamma irradiation dose [20 and 50 KGy]. The irradiated mixture had been mixed with curing agent (cycloaliphatic polyamine) at ratio of [2: 1] by using magnetic stirrer, and degassed by ultrasonic to remove the air bubbles. For prepared of epoxy/ABS/ MgOnanocomposites, different weight percentages of MgO nanoparticles (2, 5, 7, 10 %) were added to blend mixture, and the mixture was degassed and espoused to Gamma – irradiation at 20, 50 kGy by using a Co - 60 radiation source, then hardener was

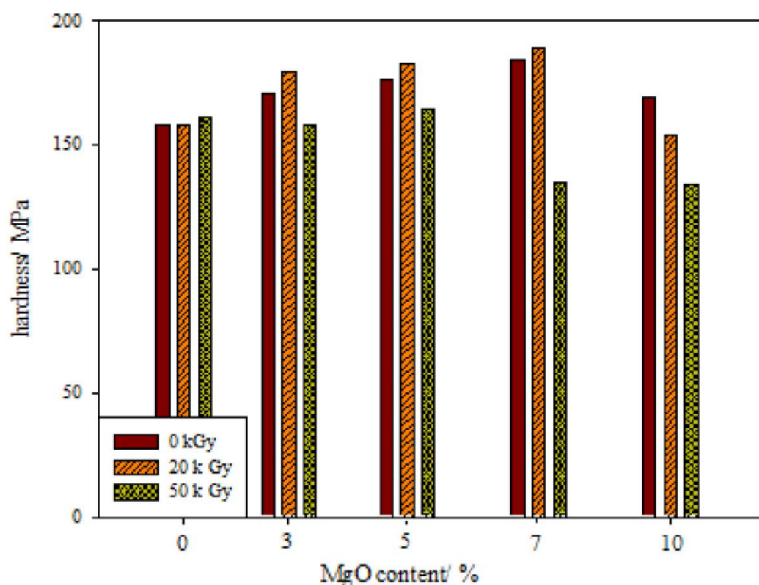


Figure 1 : Effect of MgO content on micro-hardness of unirrad. and irradiated epoxy/ ABS blend

## Full Paper

added at desired ratio.

### Mechanical properties

#### Vickers hardness test

Micro-hardness (HV) tested (Shmadzu Micro-Hardness HMV-2) are performed on epoxy and its composites. The micro-indentation hardness was measured from the residual impression of a Vickers square-based diamond indenter after an indentation time of 30 s using a load of 100 kgf.

The average of the five different points served as the reported surface hardness of the micro-hardness specimen. The Vickers hardness is the quotient obtained by dividing the kgf load by the square mm area of indentation.

$F =$  Load in kgf

$d =$  Arithmetic mean of the two diagonals,  $d_1$  and  $d_2$  in mm

HV = Vickers hardness

$$HV = [2F \sin 136^\circ/2] / d^2 \quad (1)$$

$$HV = 1.854 F / d^2 \text{ approximately} \quad (2)$$

#### Thermogravimetric analysis (TGA)

The thermogravimetric analysis (TGA) technique was applied using TG-50 instrument from Shmadzu (Japan). The heating was carried out at temperature range from 23 oC to 600 oC with a heating rate of 10 oC/ min under nitrogen gas atmosphere

#### Differential scanning calorimeter (DSC)

The glass transition temperatures (Tg) of epoxy/ABS – MgOnanocomposites were determined using a Perkin-Elmer, Diamond DSC. The measurements were performed using 5.0 mg of the samples in nitrogen atmosphere using heating rates of 10 [C/min] in the temperature range of 30-300 °C.

#### X-ray diffraction (XRD)

X-Ray Diffraction patterns of MgO particles and hybrid epoxy composites were obtained with XRD-DI series, Shimadzu apparatus using Ni-filter and Cu-K target.

## RESULTS AND DISCUSSION

### Mechanical properties

The micro-hardness technique has been established as a means of detecting a variety of morphological and textural changes in crystalline polymers and has been extensively used in research. This is because micro-indentation hardness is based on plastic straining and, consequently, is directly correlated to molecular and super-molecular deformation mechanisms occurring locally at the polymer surface. These mechanisms critically depend on the specific morphology of the material. The fact that crystalline polymers are multi-phase materials has prompted a new route in identifying their internal structure and relating it to the resistance against local deformation (micro-hardness)<sup>[16]</sup>. Figure 1 shows the micro-hardness of unirradiated and irradiated EP/ABS blend with different MgO content. The micro-hardness increase with increasing MgO loading until 7wt % then tends to stability at higher contents. It was observed that, at the same content of MgO, the irradiated samples at 20 kGy gave the highest values of micro-hardness. The addition of MgO induces a significant increase in micro-hardness with respect to neat blend matrix. Because of the large surface area of nanomaterials, opportunities will be more for physical or chemical bonding with epoxy resin, thereby enhance the interfacial bonding of particles and substrate which would lead to improved properties of the nanocomposite<sup>[17]</sup>.

#### Thermal gravimetric analysis [TGA]

Thermal stability of unirradiated and irradiated epoxy/ABS blend, and modified MgOnanocomposites was studied by TGA and DTG, which are shown in (Figures 3. a,b&c). The mass loss percentage of the composites at different temperatures and rate of thermal degradation at  $T_{max}$  was taken and is given in TABLE 1. The mass-loss curves of unirradiated blend and modified blend nanocomposites show a mainly one-step degradation between 330 – 500°C. This attributed to the thermal degradation of the cured epoxy/ABS compound. While the mass loss percentage under 300 °C ranging from 9 to 22 %, which might be due to volatilizing simple gases such as water and ammonia. It can be seen that, the weight loss curves of irradiated specimens at 20 kGy show two steps degradation the

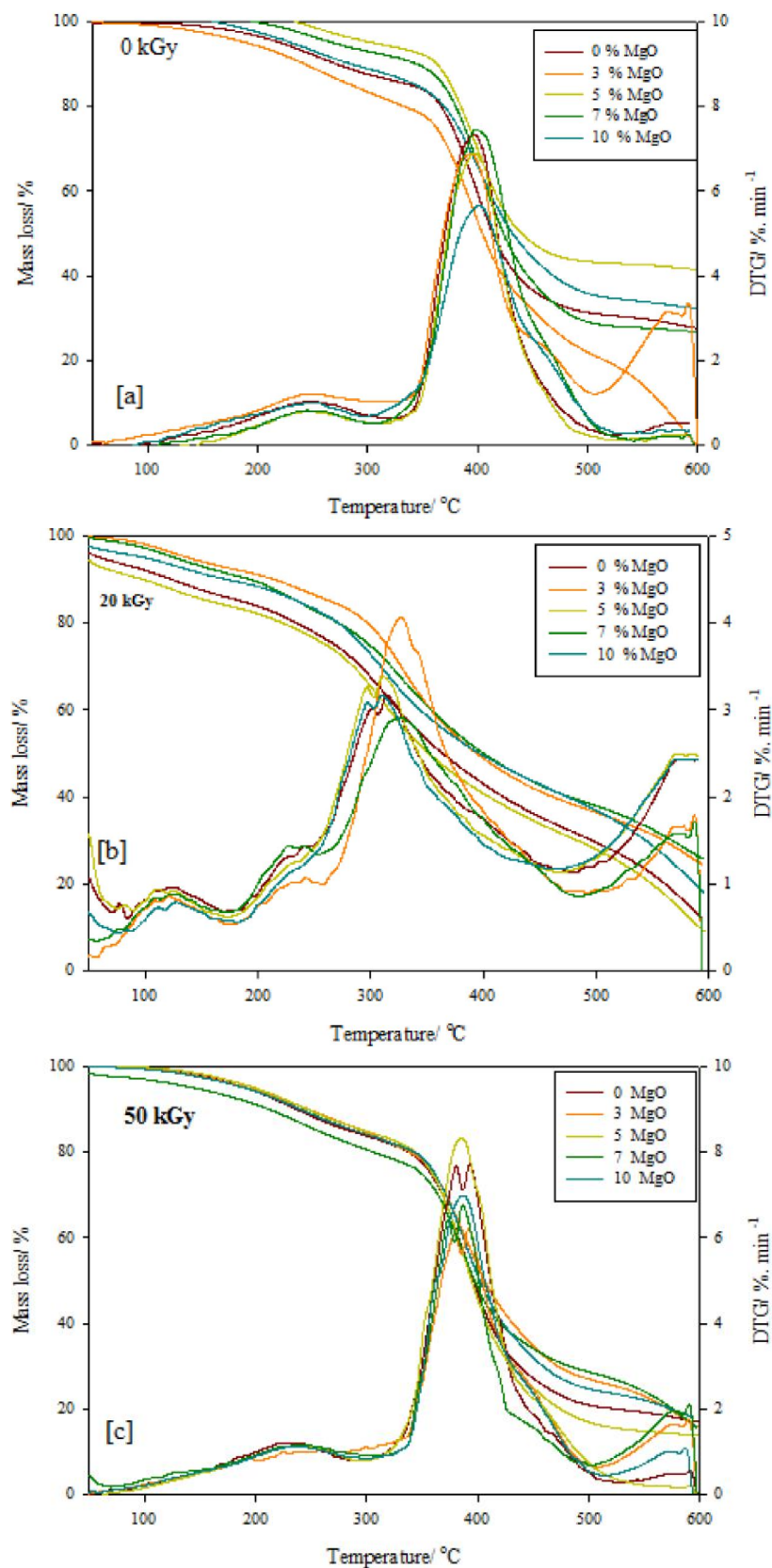


Figure 2a,b & c : TGA and derivative DTG curves of unirradiated and irradiated epoxy/ ABS blend reinforced with MgO at 20 and 50 KGy

## Full Paper

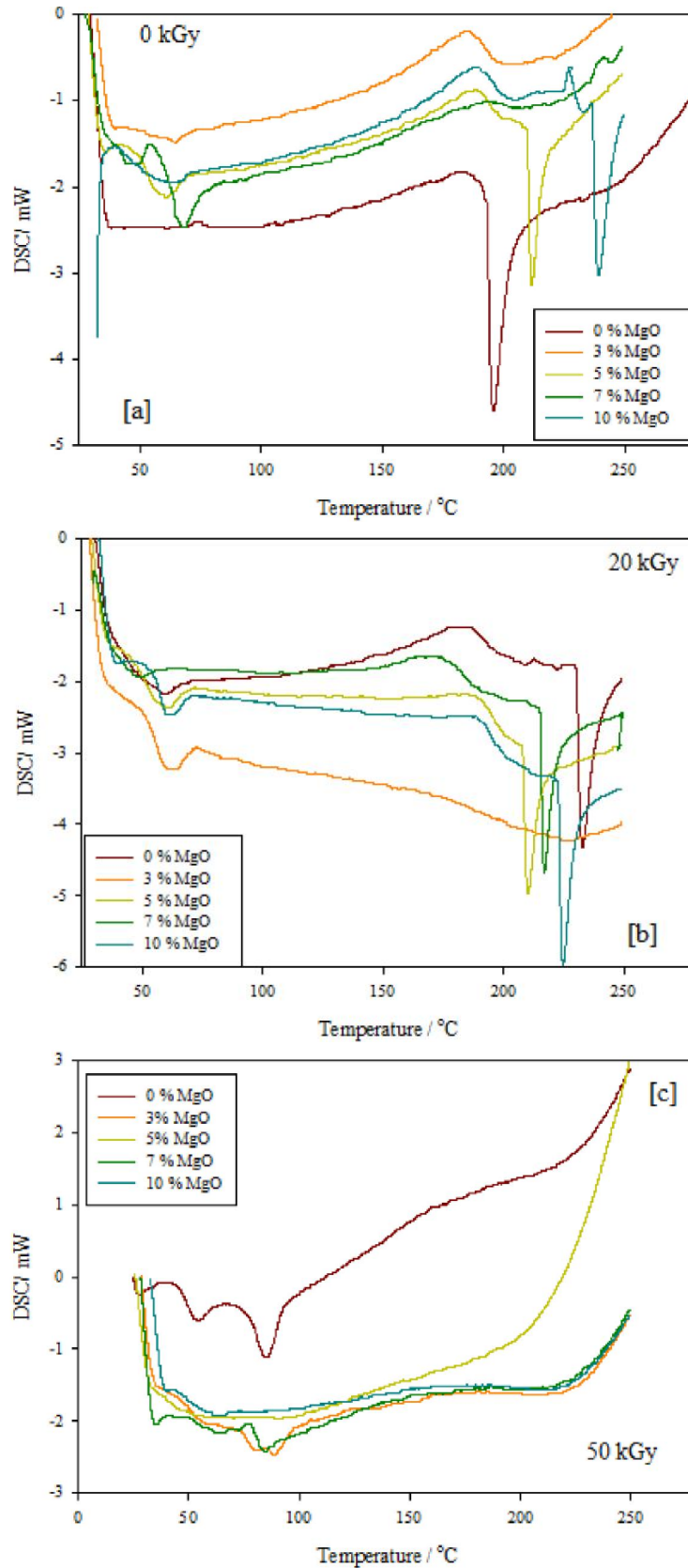


Figure 3a,b & c : DSC curves of unirradiated and irradiated epoxy/ABS blend reinforced with MgO at 20 and 50 KGy

TABLE 1 : TGA and DTG data for unirrad and irradi. epoxy/ ABS blend reinforced with MgO

Irradiation dose/ kGy	MgO load/ %	T <sub>5 wt%</sub> /°C	T <sub>10 wt%</sub> /°C	T <sub>onset</sub> /°C	T <sub>offset</sub> /°C	T <sub>max</sub> /°C	dw/dt at T <sub>max</sub> / % min <sup>-1</sup>
0	0	222	262	332	477	396	7.3
	3	192	244	331	500	396	6.9
	5	302	360	354	482	396	6.8
	7	268	344	350	495	402	7.4
	10	227	285	349	506	401	5.7
20	0	60	124	256	359	313	3.1
	3	141	213	270	466	326	4.1
	5	49	101	257	360	314	3.2
	7	130	197	264	471	326	2.9
	10	95	176	251	355	309	3.2
50	0	191	237	346	443	380	7.6
	3	195	248	345	465	385	6.1
	5	200	251	340	467	385	8.3
	7	149	212	344	431	385	6.7
	10	190	241	349	463	389	6.9

first between (250 – 360 °C) and the second between (500 – 600 °C) (Figure 2b). From thermal degradation curves of irradiated composites at 50 kGy (Figure 3c), it was observed that, the value of volatilizing simple gases that decompose under 300 °C were around 18 – 24 % while at 20 kGy range between (12 -27%). The rate of thermal decomposition of unirradiated and irradiated samples at T<sub>max</sub> was obtained from DTG curves, the data obtained were tabulated in TABLE 1. The rate of thermal decomposition of unirradiated samples decrease with increasing MgO ratio, and the irradiated samples at 20 kGy had been lowest value (TABLE 2). The change in behavior between unirradiation and irradiated hybrid composites is due to the effect of irradiation on curing and interaction between components of composites. According to prior studies, gamma-ray irradiation to polymer materials in air changes the polymer structure and produces peroxides by oxidation reaction<sup>[18]</sup>.

### Differential scanning calorimetry (DSC)

Differential scanning calorimeter (DSC) has been widely applied to the study of many phenomena occurring during a thermal scan of nano-fillers and polymer nanocomposites, such as melting, crystallization, cure kinetics, and glass transition. These properties present a peculiar change when disper-

sion at nanoscale is achieved. DSC has been applied in the investigation of numerous phenomena occurring during thermal heating of unirradiated and irradiated epoxy/ ABS and hybrid composites, including glass transition temperature (T<sub>g</sub>), vaporization temperature (T<sub>vap</sub>), and enthalpy (ΔH). (Figures 3a, b, & c) shows typical dynamic DSC curves for unirradiated and irradiated epoxy/ABS blend modified with (0, 3, 5, 7 and 10 wt %) MgO. The obtained DSC curves, as presented in Figures 3a, b, & c, showed a glass transition at ranging between 61 – 68 °C for unirradiated, consistent with the expected results for an epoxy resin. The results also showed an additional endothermic transition around 200 °C and sharp endothermic peak at above 200 °C, indicative of a ABS resin. That endothermic sharp peak disappears with irradiated specimens at 50 kGy. As indication to cross-linking of polymers blend in addition to compatibility with each other. The glass transition (T<sub>g</sub>), the vaporization temperature (T<sub>vap</sub>) and ΔH of unirradiated and irradiated composites has been determined from DSC curves (Figure 3a, b & c), and is given in TABLE 2. From data, it seen that, the vaporization temperature (T<sub>vap</sub>) of unirradiated nanocomposite increase with increasing MgO content due to the positive effect of MgO on thermal stability while ΔH of unirradiated [0, 5 and

## Full Paper

TABLE 2 : Glass transition temperature ( $T_g$ ), crystallinity ( $T_{Cryst}$ ) and ( $\Delta H_{Cryst}$ ) of Epoxy/ABS blend reinforced with MgO

Irradiation dose/ kGy	MgOload/ %	$T_g/ ^\circ C$	$T_{vap.}$	$T_C/ ^\circ C$	$\Delta H_C/ Jg^{-1}$
0	0	61	----	195	9.56
	3	62	199	220	----
	5	62	198	212	3.98
	7	68	205	242	----
	10	64	202	239	2.75
20	0	60	197	233	6.2
	3	60.7	203	----	----
	5	61.6	200	210	7.2
	7	48.2	190	217	10.4
	10	60.3	204	225	8.4
50	0	51	227	----	----
	3	79	225	----	----
	5	71	211	----	----
	7	73	223	----	----
	10	65	224	----	----

10 wt % MgO] were 9,56, 3,98 and 2,75 respectively TABLE 2. It can observe that, the enthalpy  $\Delta H$  for irradiated nanocomposites at 20 kGy increase with increasing MgO content, and the  $T_{vap.}$  of unmodified composite was higher than unirradiated composite, meanwhile the  $T_{vap.}$  of hybrid composites EP/ABS/MgO less than those unmodified. This may attributed to crosslinked of polymer blend and interaction with MgO particles with polymer matrix.

### X-ray diffraction

Figure (4, 5) shows the X-ray diffraction patterns of epoxy, epoxy/ABS and epoxy/ABS/MgO composites before and after irradiation respectively. It can be seen that, the composites contains epoxy, ABS and minor amounts of MgO, respectively. The amorphous phases identified by XRD are in agreements with the results obtained. XRD pattern of the epoxy before irradiation has big hump ( $\theta = 8.9$  to  $30$ ) with organically and disappear with addition of ABS ratio (Figure 4). This related to the crosslink between atoms in network of composite and increases the ratio of crystallinity. Meanwhile, in this Figure but after irradiation show that interoperation between atoms increase with MgO ratio and become partially crystalline. Addition the organically modified epoxy/ABS (irradiated) showing a strong reflection

peak with the characteristic d-spacing distance that shifted towards smaller angles was observed. The interlayer spacing of epoxy/ABS (irradiated) composites were found to be higher than the epoxy and epoxy/ABS (un- irradiated). The increase in the interlayer spacing of epoxy/ABS (un- irradiated) and epoxy/ABS (irradiated) was due to the presence of alkylammonium ions at gallery regions<sup>[19]</sup>. XRD pattern (Figure 4,5) of the epoxy/ABS/MgO composites before and after irradiation organically modified MgO particles show that the intensity increase with additive the MgO and appeared sharp beak at ( $\theta=14.5^\circ$ ) and small beak at ( $\theta=9^\circ, 16.5^\circ, 28^\circ$ ) but after applied irradiation the beak become more sharp and the composites become crystallinity. This indicated that the MgO has improve the structure of composites, become homogeneity and moved from exfoliated region to intercalated region, i.e., the interlayer spacing distance of the MgO has been decreased which Bragg's law. The excess of orientation of the MgO layers confirms the complete intercalated of the MgO platelets within the epoxy/ABS systems.

The data of XRD spectra were compared with theoretical data using JCPDS (joint committee on powder diffraction standards)<sup>[20]</sup> for the epoxy/ABS, epoxy/ABS/MgO composites. The values of

TABLE 3 : Calculated values of crystallite size (L) and number of crystallites per unit area( $m^2$ ) forepoxy/ ABS blend reinforced with MgO

Irradiation dose/ kGy	MgO load/%	2Theta ( $2\theta$ )	Intensity	lattice spacing (d)	FWHM (Radian)	Crystal size(L)	No. of crystallites per unit area( $m^2$ )
0	0	19.11333	124.3333	4.640243	-----	-----	-----
	3	19.13193	219.6667	4.635773	156.0935	0.008731	1589.003
	5	16.44483	85.33333	5.386719	58.27141	0.028244	119.5784
	7	17.97333	112.3333	4.931912	-----	-----	-----
	10	18.92353	240.3333	4.686354	222.2002	0.00616	4584.466
50	0	18.88667	190.3333	4.695418	33.3284	0.041135	15.08513
	3	16.75333	171.3333	5.288214	50.87575	0.028418	61.29401
	5	13.49177	411	6.558395	89.64573	0.016187	344.7156
	7	13.49873	450.3333	6.555026	85.1647	0.016893	286.6664
	10	13.37	290.6667	6.617851	78.72268	0.01824	222.7432

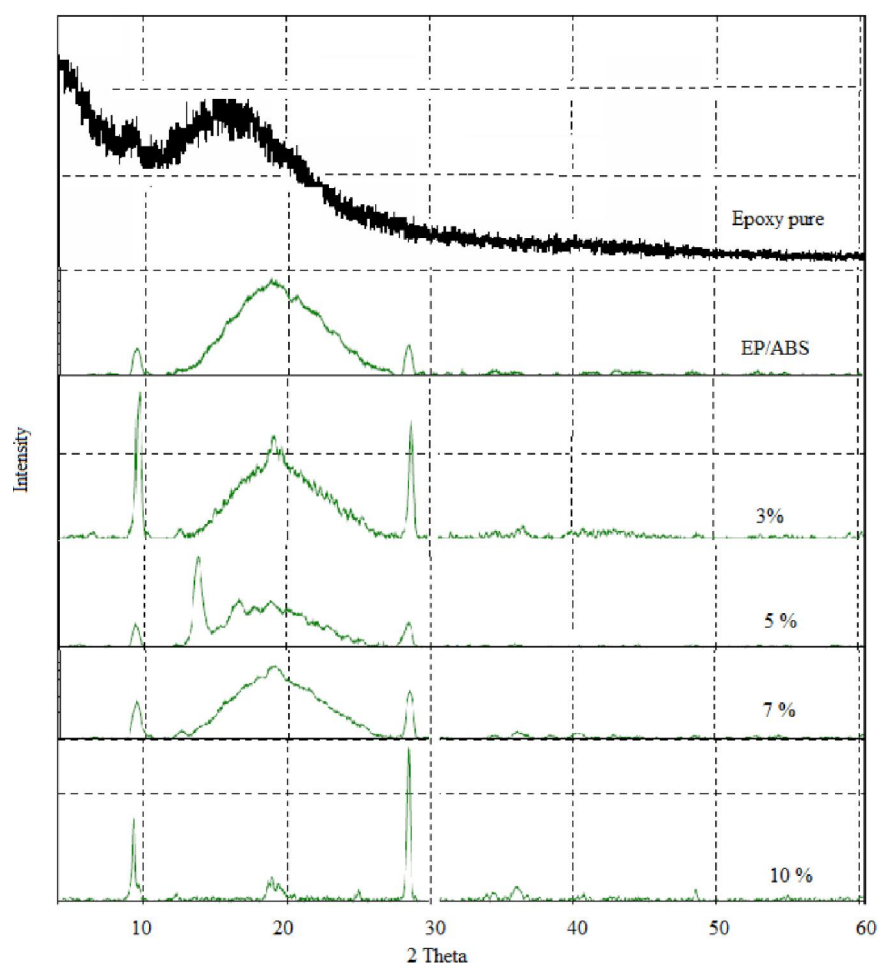


Figure 4 : XRD patterns of unirradiated. epoxy and epoxy/ABS blend reinforced with different MgO load

2Theta ( $2\theta$ ), Intensity, FWHM (Radian), Crystal Size (L) and number of crystallites per unit area ( $m^2$ ) for epoxy/ABS, epoxy/ABS/MgOcomposites before and after irradiation were given in TABLE 3. There was no any information available for  $hkl$  crystal planes

(Miller indices) for the epoxy/ABS/MgOcomposites in JCPDS calculated data. It is clear from TABLE 3 that the angle ( $2\theta$ ), percentage intensity, and lattice spacing ( $d$ ) are in close agreement with each other. The experimental lattice spac-

## Full Paper

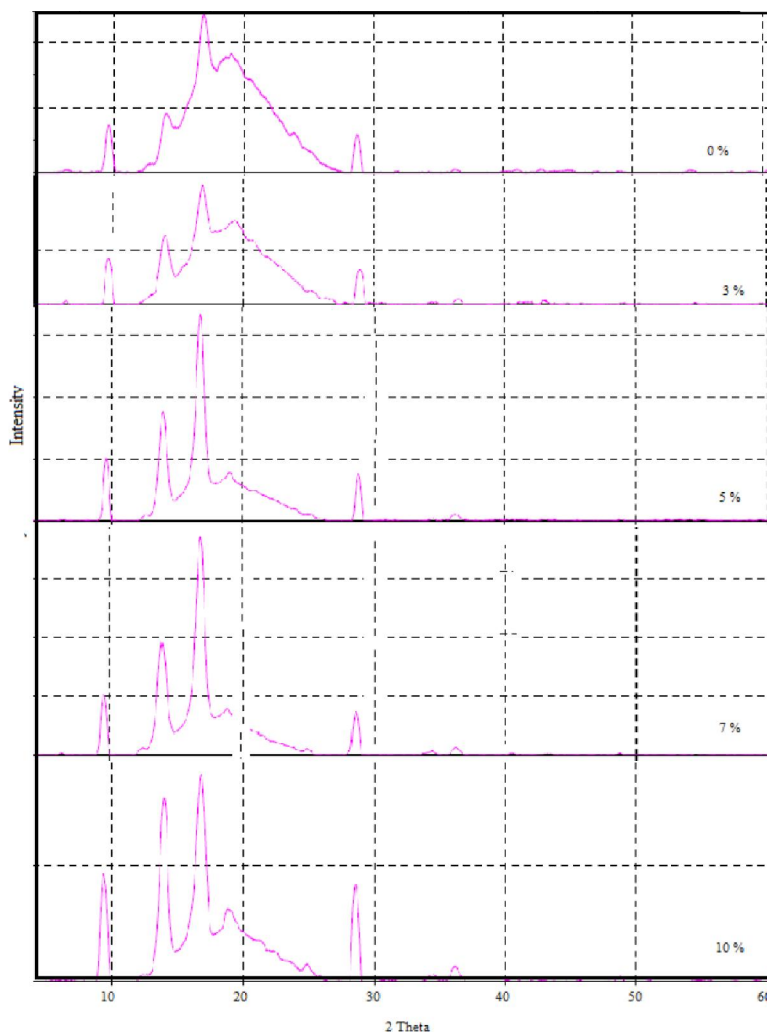


Figure 5 : XRD patterns of irradiated epoxy/ABS blend reinforced with different MgO load at 50 kGy

ing (d) was calculated using Bragg's law ( $2d \sin \theta = n\lambda$ ) for the composites. It shown that shift to increase after irradiation samples, which indicates that lattice parameters change; in other words, there is phase change in the material after irradiation. It is clear from the table that the intensity of XRD peaks for irradiated samples increases followed by an increase in the ratio of MgO. The amorphization is due to disordering of the polymeric chains, which further depends upon LET of the incoming ion and chemical nature as well as the geometrical structure of the polymeric chains<sup>[21]</sup>. The irradiation and ratio also affected on crystallite size and number of crystallites per unit area. The average crystallite size ( $L$ ) is calculated by using the Scherrer formula<sup>[22]</sup> as given in the following equation:

$$L = K\lambda / (\beta \cos \theta) \quad (3)$$

Where  $\beta$  is the FWHM of the peak (in rad).  $\lambda$  is the wavelength of the X-rays used ( $1.54 \text{ \AA}$  for Cu  $K\alpha$  radiation),  $\theta$  (in deg) is the angle which is calculated by taking  $1/2$  of  $2\theta$  value as indicated in (Figure 4, 5).  $K$  is a constant of proportionality (the Scherrer constant); its value depends on various factors such as the width, the shape of the crystal, and the size distribution. The value of  $K$  is 0.9 for FWHM of spherical crystals with cubic symmetry<sup>[23]</sup>.

And Number of crystallites per unit area is calculated by using formula<sup>[24]</sup> as given in the following equation:

$$(N) = t/L^3 \quad (4)$$

where  $t$  is the thickness of the sample. From the data of the crystallite size ( $L$ ) it show that ( $L$ ) increases with increase the ratio of MgO after irradiation but before irradiation it shown that the ratio (zero, 7)

TABLE 4 : Calculated Values of XRD Parameters for unirrad. and irradiated epoxy/ ABS blend reinforced with MgO

Irradiation dose/ kGy	MgO load/%	Inter chain separation (R)	interplanar distance (d)	microstrain ( $\epsilon$ )	dislocation density ( $\delta$ )	distortion parameters (g)
0	0	0.159709	0.127767	-----	-----	-----
	3	0.159497	0.127598	25.55533	13165.57	1223.01
	5	0.137563	0.110051	14.44684	2093.649	454.0453
	7	0.150267	0.120214	-----	-----	-----
	10	0.157777	0.126221	54.67613	26626.61	1672.088
50	0	0.157825	0.12626	8.241741	590.9806	224.46
	3	0.140122	0.112098	12.60698	1439.729	385.5879
	5	0.112966	0.090373	22.26403	4492.472	848.8412
	7	0.113024	0.090419	21.15008	4013.281	803.9196
	10	0.11195	0.08956	19.55253	3411.864	750.2442

there are no crystallite size ( $L$ ) because there are dependent on  $FWHM(\beta)$ . The increase in the crystallite size ( $L$ ) indicates a decrease in amorphous of the epoxy/ABS and increase in crystallinity after additive the MgO and irradiation. In the fact, the epoxy pure is amorphous, but after additive (ABS, MgO) become composites and change in structure. There are appeared sharp peaks with increase the ratio of MgO and after irradiation. The composites become partially crystalline. There are other factors such as interchain separation ( $R$ ), interplanar distance ( $d$ ), microstrain ( $\epsilon$ ), dislocation density ( $\delta$ ), and distortion parameters ( $g$ ) are also calculated using following equations<sup>[25-27]</sup>:

$$R = 5\lambda/8 \sin\theta \quad (5)$$

$$d = \lambda/2 \sin\theta \quad (6)$$

$$\epsilon = b \cos \theta/4 \quad (7)$$

$$\delta = 1/L^2 \quad (8)$$

$$g = b/ \tan \theta \quad (9)$$

These parameters are calculated and given the data in TABLE 4. The table indicates that there is few change in the interchain separation ( $R$ ) and interplanar distance ( $d$ ) for all ratio before irradiation except the ratio 5, but after irradiation the values are decrease. This are related to ( $2\theta$ ) where it decrease with increase the ratio of MgO and the behavior of samples change by exposure to irradiation. The parameters micro-strain ( $\epsilon$ ), dislocation density ( $\delta$ ), and distortion parameters ( $g$ ) show a variations in values of before and after irradiation for all samples excepts the ratio (zero,7) because all parameters dependence on the  $FWHM(\beta)$ .

## CONCLUSION

Epoxy/ABS – MgO nanocomposites had been prepared by exposure epoxy/ABS mixture to gamma irradiation dose (20 – 50 kGy), and MgO particles was added mixture at different wt percentage. then added the hardener to hybride mixture to cure at room temperature. The microhardness. The micro hardness increase sharply with increasing MgO loading until 5 wt % then tends to stability at higher contents. The weight-loss curves of unirradiated and irradiated blend and modified blend nanocomposites show a mainly one-step degradation between 330 – 490 °C. the rate of thermal decomposition of irradiated composites less than unirradiated composite, and for unirradiated samples the rate of thermal decomposition decrease with increasing MgO content. the crystallization temperature ( $T_{vap.}$ ) of unirradiated nanocomposite increase with increasing MgO content due to the positive effect of MgO on thermal stability while  $\Delta H$  of unirradiated [0, 5 and 10 wt % MgO] 9,56, 3,98 and 2,75 Jg<sup>-1</sup> respectively. XRD pattern of the epoxy/ABS/MgO composites before and after irradiation show that the intensity increase with additive the MgO and appeared sharp peak at ( $\theta=14.5^\circ$ ) and small peak at ( $\theta=9^\circ, 16.5^\circ, 28^\circ$ ) but after applied irradiation the peak become more sharp and the composites become crystalline.

## REFERENCES

- [1] J.K.Fink, Epoxy Resins; Reactive polymers Funda-

## Full Paper

- mentals, and Applications, William Andrew: Norwich, NY, 240 (2005).
- [2] A.J.Kinloch; Adhesion and adhesive science and technology; Chapman Hall: London, (1987).
- [3] J.T.Carter, G.T.Emmerson, C.L.Faro, P.T.McGrail, D.R.Moore; Compos.Part A Appl.Sci.Manuf., **80**, 83 (2003).
- [4] G.Almen, R.M.Byrens, P.D.Mackenzie, R.K.Maskell, P.T.McGrail, M.S.Sefton; 34th International SAMPE Symposium, Society for the Advancement of Material and Process Engineering, California, USA, **34**, 259 (1989).
- [5] P.Jyotishkumar, J.Pionteck, R.H€aßler, S.M.George, U.Cvelbar, S.Thomas; Ind.Eng.Chem.Res., **50**, 4432 (2011).
- [6] B.Wetzel, P.Rosso, F.Hauptert, K.Friedrich; Eng.Fract.Mech., **73**, 2375 (2006).
- [7] Girard E.Reydet, C.C.Riccardi, H.Sautereau, J.P.Pascualt; Macromolecules, **28**, 7608 (1995).
- [8] L.Mangeng, K.Sangwook; J Appl.Polym.Sci., **71**, 2401 (1999).
- [9] L.Barral, J.Cano, Lo'J.pez, Lo'pez I.Bueno, P.Nogueira, M.J.Abad, C.Ram' rez; Polymer 1999, in press.
- [10] A.Chapiro; Radiation chemistry of polymeric systems, Interscience Publishers, New York, (1962).
- [11] T.Özdemir, A.Usanmaz; Radiat.Phys.Chem., **77**, 799 (2008).
- [12] V.Lopata, C.B.Saunders, A.Singh, C.J.Janke, G.E.Wrenn, S.J.Havens; Radiat.Phys.Chem., **56**, 405 (1999).
- [13] A.Singh, J.Silverman; Editions, Radiation processing of polymers, Carl Hanser, Munich, (1992).
- [14] A.Singh, C.B.Saunders, J.W.Barnard, V.J.Lopata, W.Kremers, T.E.McDougall, M. hung, M.Tateishi, Ali A.M. Yassene; Effect of gamma irradiation on physico - mechanical properties of epoxy /polyacrylonitrile-butadiene-styrene blend, The 5<sup>th</sup> International Conference on Structural Analysis of Advanced Materials, 23-26 September, Kipriotis Village Resort, Island of Kos, Greece, (2013).
- [15] F.J.BaltáCalleja, S.Fakirov; Microhardness of polymers, Cambridge University Press, (2000).
- [16] P.Jyotishkumar, P.Ju' rgen, M.Paula, T.Sabu; J.Appl.Polym.Sci., **127**(4), 3159–3168 (2013).
- [17] K.Y. Kim, D.S.Im, J.H. Choi, K. Y. Lee; Degradation properties of the epoxy nanocomposite caused by a gamma-ray irradiation, 2010 Annual Report Conference on Electrical Insulation and Dielectric Phenomena.
- [18] M.Suguna Lakshmi a, B. Narmadha b, B.S.R. Reddy, Polymer Degradation and Stability 93 (2008) 201-213.
- [19] Wong W.Ng, H.F.McMurdie, C.R.Hubbard, A.D.Mighell; J.Res.NatlInst Stand Technol., **106**, 1013–1028 (2001).
- [20] V.R.Gowariker, N.V.Viswanathan, Sreedhar; Polymer Science; New Age International: India, (2002).
- [21] A.L.Patterson; Phys.Rev., **56**, 978–982 (1939).
- [22] J.I.Langford, A.J.C.Wilson; J.Appl.Crystallogr, **11**, 102–113 (1978).
- [23] M.B.OrtuñoLópez, J.J.Valenzuela-Jáuregui, M.Sotelo-Lerma, A.Mendoza-Galván, R.Ramirez-Bon; Thin Solid Films, **429**, 34-39 (2003).
- [24] B.Mallick, T.Patel, R.C.Behera, S.N.Sarangi, S.N.Sahu, R.K.Choudhar; NuclInstrum Methods Phys.Res., Sect B, **248**, 305 (2006).
- [25] M.Madani; Curr.Appl.Phys., **11**, 70 (2011).
- [26] A.Vij, A.K.Chawla, R.Kumar, S.P.Lochar, R.Chandra, N.Singh, Physica B, **405**, 2573–2576. (2010).